Proceedings of the Sixth International Conference on
Railway Technology: Research, Development and Maintenance
Edited by: J. Pombo
Civil-Comp Conferences, Volume 7, Paper 4.10
Civil-Comp Press, Edinburgh, United Kingdom, 2024
ISSN: 2753-3239, doi: 10.4203/ccc.7.4.10

A Simplified Modal Superposition Method Based Pantograph-Stitched Catenary Interaction Model

Y. Xu[1], H. Li[2], J. Lei[1] and W. Z. Liu[3]

[1]Faculty of Transportation Engineering, Kunming University of Science and Technology, Kunming, China
[2]State Key Laboratory of Rail Transit Vehicle System, Southwest Jiaotong University, Chengdu, China
[3]Department of Engineering Mechanics, KTH Royal Institute of Technology, Sweden

Abstract

The modal superposition method (MSM) has been proven to be more accurate and more efficient than the finite element method in modeling pantograph-catenary interaction systems. However, the stitched wire in a stitched catenary system is difficult to directly model by the modal superposition method, which limits its application in the investigation of pantograph-stitched catenary interaction dynamics. In this work, a new modal superposition method-based pantograph–stitched catenary interaction model is developed to simulate pantograph–stitched catenary interactions. In this model, the stitched wire is simplified into a part of the messenger wire supported by two spring-damping elements, and the modal superposition method is then used to model the simplified stitched catenary system. The present model is validated by the EN 50318:2018 standard. The validation results show that the proposed modal superposition method-based model can accurately simulate the pantograph-stitched catenary interaction with proper key parameters considered, including the distance between every two spring-damper elements and the stiffness of the elements.

Keywords: stitched catenary, modal superposition, stitch wire model, pantograph-catenary interaction, EN50318:2018 standard, calculation efficiency.

1 Introduction

The pantograph–catenary dynamics directly affect the current-collection quality and maintenance costs [1] of electrified railways. Poor pantograph–catenary dynamics can

cause excessive wear, damage pantograph contact strips and contact wires [2,3], and limit operational speed [4,5]. The high-speed train operation speed continues to increase in many countries, and the increasing train operation speed makes the dynamic characteristics of the pantograph-catenary system more complex. To maintain the current-collection quality and increase the operational reliability, it is necessary to investigate the dynamic behavior of the high-speed pantograph-catenary interaction system.

Many researchers have investigated pantograph–catenary dynamics from different perspectives. While simple pantograph–catenary interaction cases have been previously studied [6–9], more complicated situations, such as multi pantograph operation [10–13] and the influence of various environmental factors on pantograph–catenary interactions [4,14,15], have been investigated. The finite element method (FEM) and modal superposition method (MSM) are widely used in these studies to model pantograph-catenary interaction systems. The FEM can model the complex structure of a catenary, but its corresponding number of degrees of freedom (DOFs) is large, and its calculation efficiency is limited. Yang et al. [10] investigated the wind deflection of a catenary under crosswind, where the catenary system is modeled by absolute nodal coordinate formulation. Massat et al. [11] developed a pantograph-catenary interaction model to optimize its dynamic behavior in France, where the catenary system is modeled by FEM. Tur et al. [12] developed an absolute nodal coordinate FEM-based catenary model to compute its initial configuration. The MSM can capture the main dynamic characteristics of the catenary system and can model the catenary system with fewer DOFs. Thus, its calculation efficiency is greater than that of the FEM. Facchinetti and Bruni [13] developed a real-time catenary model to efficiently simulate the pantograph-catenary interaction in the hardware-in-the-loop case, where the catenary system is reduced and modeled by MSM. Ronnquist and Navik [14] analyzed the frequency characteristics of a catenary system to explore higher train velocities. Facchinetti et al. [15] further optimized the real-time catenary model to achieve higher calculation efficiency.

It can be seen from the above investigations that the MSM can efficiently and accurately investigate the dynamics of the pantograph-catenary system. However, the existing MSM-based models only consider simple catenary systems, and stitched catenary systems are ignored. This is mainly caused by the fact that the shape function of the stitch wire connecting with the messenger wire at the end of every two neighboring spans is difficult to express. Because the stitched catenary system is widely applied in high-speed railway systems [16], the application of the MSM in high-speed pantograph-catenary interaction dynamic studies is limited.

In this study, a new MSM-based pantograph–stitched catenary interaction model is developed to accurately and efficiently simulate pantograph–stitched catenary interactions. In this model, the stitch wire and catenary suspension are simplified into a part of the messenger wire supported by a couple of spring-damper elements, where the distance of these two spring-damper elements and the stiffness of each spring-damping element are chosen to ensure that the stiffness of the stitch wire model is equal to the original stiffness. Then, the stitched catenary system with a simplified

stitch wire model is modeled by MSM. After the formulation of the present model, it is validated by the EN 50318-2018 standard, and the influence of different key parameters in the stitch wire model on calculation accuracy is investigated. The remainder of this paper is organized as follows. The proposed MSM-based pantograph–stitched catenary interaction model is formulated in Section 2, and it is validated in Section 3. Finally, conclusions based on this study are presented in Section 4.

2 Methods

In the stitched catenary system, the stitch wire is designed to optimize the stiffness of the catenary structure near the registration arms, which can further optimize the dynamic performance of the pantograph-catenary interaction. The stitch wire is located above the registration arms and connects to the messenger wire and dropper, as shown in Fig. 1(a). Note that the function of the stitch wire is similar to that of the messenger wire, which also has tension and carries the contact wire through the dropper. The stitch wire is also supported by the messenger wire through the clamp. Therefore, the stitch wire can be simplified to a part of the messenger wire at the same location to carry the contact wire through the dropper. The catenary suspension is then combined with the original messenger wire above the stitch wire and modeled by a couple of spring-damping elements to further support this part of the messenger wire, as shown in Fig. 1(b). This part of the messenger wire and spring-damping elements form the stitch wire model. Because the stitch wire is simplified, the MSM can be further extended to the stitched catenary system. The detailed modeling processes are shown below.

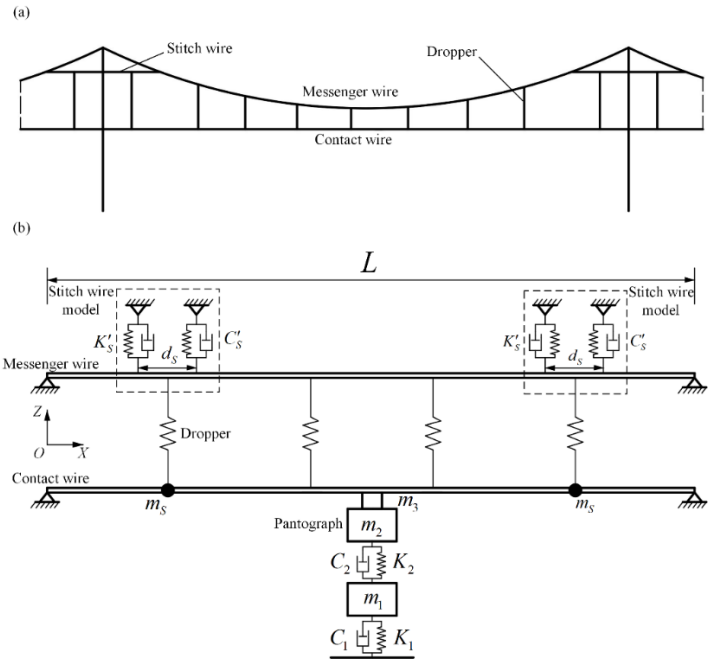

Figure 1: Schematic of the pantograph–stitched catenary interaction system: (a) stitched catenary system and (b) present pantograph–stitched catenary interaction system.

The stitch wire model is first modeled. As mentioned above, the stitch wire is simplified to a part of the messenger wire, and the catenary suspension and the original messenger wire are modeled as a couple of spring-damping elements. The distance between these two spring-damper elements is d_S, and the stiffness and damping of these two elements are K_S' and C_S', respectively. These values are chosen to ensure that the stiffness of the catenary at the stitch wire part is equal to the original stiffness. The dynamic force of the spring-damping elements can be calculated by

$$F_S = K_S' d_S + C_S' \dot{d}_S \tag{1}$$

where d_S is the displacement of the messenger wire at the location of the spring-damping elements. These key values can be determined by the pre-analysis method [17].

The messenger wire and contact wire are then modeled. Both the contact and messenger wires are considered Euler–Bernoulli beams, and the stitch wire is considered as a part of the messenger wire with a couple of spring-damping elements supporting this part, which makes the structure of the present stitch catenary model familiar to the simple catenary system. Based on the MSM, the dynamic equations of the contact and messenger wire are

$$\mathbf{M}_m \ddot{\mathbf{q}}_m + \mathbf{C}_m \dot{\mathbf{q}}_m + \mathbf{K}_m \mathbf{q}_m = \mathbf{Q}_{flowm} + \mathbf{Q}_{Fm} \tag{2}$$

$$\mathbf{M}_c \ddot{\mathbf{q}}_c + \mathbf{C}_c \dot{\mathbf{q}}_c + \mathbf{K}_c \mathbf{q}_c = \mathbf{Q}_{flowc} + \mathbf{Q}_{Fc} \tag{3}$$

where $\mathbf{M}_m$, $\mathbf{C}_m$, and $\mathbf{K}_m$ are the mass, damping, and stiffness matrices of the messenger wire, respectively, and $\mathbf{M}_c$, $\mathbf{C}_c$, and $\mathbf{K}_c$ are the mass, damping, and stiffness matrices of the contact wire, respectively. $\mathbf{Q}_F$ is the generalized force vector generated by the force acting on the wire, such as the pantograph-catenary interaction force. The expression of these matrices can be found in [17].

The dropper and registration arm are finally modeled. Based on (), the dropper is modeled as bilinear spring elements with only the stretch stiffness considered, and the registration arm is modeled as a lumped mass m_S attached to the contact wire. Details of these models are shown in [17].

Based on the dynamic equations of the messenger and contact wires, the stitch wire model, and the model of the dropper and registration arm, the stitched catenary model is finally formulated as

$$\begin{bmatrix} \mathbf{M}_m & \\ & \mathbf{M}_c \end{bmatrix} \begin{bmatrix} \ddot{\mathbf{q}}_m \\ \ddot{\mathbf{q}}_c \end{bmatrix} + \begin{bmatrix} \mathbf{C}_m & \\ & \mathbf{C}_c \end{bmatrix} \begin{bmatrix} \dot{\mathbf{q}}_m \\ \dot{\mathbf{q}}_c \end{bmatrix} + \begin{bmatrix} \mathbf{K}_m & \\ & \mathbf{K}_c \end{bmatrix} \begin{bmatrix} \mathbf{q}_m \\ \mathbf{q}_c \end{bmatrix} = \begin{bmatrix} \mathbf{Q}_{flowm} + \mathbf{Q}_{Fm} \\ \mathbf{Q}_{flowc} + \mathbf{Q}_{Fc} \end{bmatrix}. \tag{4}$$

In Eq. (5), $\mathbf{Q}_{Fm}$ is caused by the dropper force, dynamic force F_S in the stitch wire model, and messenger wire gravity. $\mathbf{Q}_{Fc}$ is caused by the dropper force, registration arm gravity, stagger forces, contact wire gravity, and pantograph-catenary contact force. Stagger forces are applied on every registration arm acting point to form the stagger of the catenary.

The pantograph is modeled as a lumped mass system model, which consists of a contact strip, panhead, frame, and spring-damper elements. Based on [18], the contact

strip, panhead, and frame are simplified as lumped masses, and the contact strip and panhead are combined and connected with the frame through spring-damper elements, as shown in Fig. 1 (b). The contact strip, panhead, and frame mass of the pantograph are m_3, m_2, and m_1, respectively. The stiffness and damping of the spring-damper elements between the panhead and frame are K_2 and C_2, respectively, and those of the spring-damper elements between the frame and car body are K_1 and C_1, respectively. The dynamic equation of the pantograph is expressed as

$$\mathbf{M}_P\ddot{\mathbf{q}}_P + \mathbf{C}_P\dot{\mathbf{q}}_P + \mathbf{K}_P\mathbf{q}_P = \mathbf{Q}_{cP} + \mathbf{Q}_P, \tag{5}$$

where $\mathbf{M}_P$, $\mathbf{C}_P$, and $\mathbf{K}_P$ denote the spring, damping, and stiffness matrices of the pantograph, respectively. $\mathbf{q}_P$ is the generalized coordinate vector, $\mathbf{Q}_{cP}$ is the generalized force vector caused by the pantograph-catenary interaction, and $\mathbf{Q}_P$ is the generalized force vector generated by the pantograph itself, which includes gravity, uplift forces, and aerodynamics. The details of these matrices are shown in [18].

Based on the present stitched catenary model and pantograph model, the MSM-based pantograph–stitched catenary interaction model can be formulated, and its dynamic equations are

$$\begin{bmatrix} \mathbf{M}_m & & \\ & \mathbf{M}_c & \\ & & \mathbf{M}_P \end{bmatrix}\begin{bmatrix} \ddot{\mathbf{q}}_m \\ \ddot{\mathbf{q}}_c \\ \ddot{\mathbf{q}}_P \end{bmatrix} + \begin{bmatrix} \mathbf{C}_m & & \\ & \mathbf{C}_c & \\ & & \mathbf{C}_P \end{bmatrix}\begin{bmatrix} \dot{\mathbf{q}}_m \\ \dot{\mathbf{q}}_c \\ \dot{\mathbf{q}}_P \end{bmatrix} + \begin{bmatrix} \mathbf{K}_m & & \\ & \mathbf{K}_c & \\ & & \mathbf{K}_P \end{bmatrix}\begin{bmatrix} \dot{\mathbf{q}}_m \\ \dot{\mathbf{q}}_c \\ \dot{\mathbf{q}}_P \end{bmatrix} = \begin{bmatrix} \mathbf{Q}_{flowm} + \mathbf{Q}_{Fm} \\ \mathbf{Q}_{flowc} + \mathbf{Q}_{Fc} \\ \mathbf{Q}_{cP} + \mathbf{Q}_P \end{bmatrix}. \tag{6}$$

In Eq. (6), $\mathbf{Q}_{Pc}$ denotes the generalized force vector of the contact wire caused by F_c. The pantograph–catenary dynamic force is calculated through

$$F_c = \begin{cases} k_n d_r, d_r \geq 0 \\ 0, d_r < 0 \end{cases}, \tag{7}$$

where k_n is the contact stiffness and d_r is the gap between the contact wire and contact strip. The k_n in the present model is 50000 N/m [18].

3 Results

The present MSM-based pantograph–stitched catenary interaction model is validated based on the EN50318-2018 standard [16], which is a European standard for pantograph–catenary interaction simulation validation of an AC stitched catenary and its corresponding pantograph. The double pantograph is considered, and the length of the catenary model is 1200 m. In the stitch wire model, the d_S is 19 m, and K_S' is 7×10^5 N/m. These two values are determined by the pre-analysis method. The number of modes considered in the modeling is n = 360. The time histories of the pantograph-catenary contact forces based on the EN50318:2018 standard are shown in Fig. 2. The corresponding statistical results are shown in Table 1. As shown in Fig. 2 and Table 1, the results from the present model are reasonable, and its corresponding statistical

results meet the demand of Table A.7 in EN50318-2018. Based on these results, the accuracy of the present MSM-based pantograph–stitched catenary interaction model can be validated, and the present stitch wire model can accurately present the dynamic behavior of the stitch wire parts.

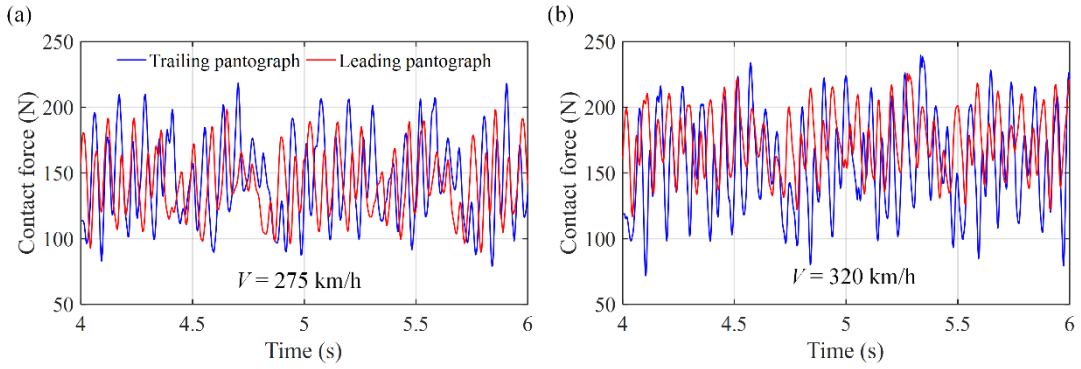

Figure 2: Time histories of the pantograph-catenary contact forces at different velocities and pantographs: (a) V = 275 km/h and (b) V = 320 km/h.

Speed [km/h]	275		320	
Pantograph	Leading	Trailing	Leading	Trailing
F_m [N]	143.1(143-144)	143.7(142-144)	169(169)	169(169)
σ [N]	24.1(20.2-24.7)	28.9(24.4-36.2)	23.2(20.5-24.7)	36.9(30.4-38.3)
σ (0 Hz-5 Hz) [N]	14.8(11.7-15.2)	17.9(17.0-18.2)	13.0(11.8-13.3)	22.9(20.4-24.2)
σ (5 Hz-20 Hz) [N]	18.5(16.5-19)	25.5(16.4-27.4)	19.1(15.2-20.9)	28.8(21.5-29.8)
Actual maximum of contact force [N]	198.5(185-199)	225.2(203-252)	229.2(210-232)	242.3(239-255)
Actual minimum of contact force [N]	95.6(92-102)	86.2(56-88)	121.4(105-128)	74.4(43-78)
Range of vertical position of the point of contact [mm]	22.4(18-25)	32.5(26-36)	21.6(13-23)	59.8(38-63)
Maximum uplift at support [mm]	68.2(55-79)	71.3(51-79)	88.6(74-95)	91.1(69-95)
Percentage of loss of contact [%]	0(0)	0(0)	0(0)	0(0)

Table 1: Statistical results of the pantograph-catenary interaction with respect to different pantographs and speeds.

The influence of the distance between every two spring-damping elements d_S and spring-damping element stiffness K_S' in the stitch wire model on the calculation accuracy are then discussed, which are the key parameters of the present stitched wire model. Based on the present validation case, the mean contact force and standard deviation of the contact force at the lead pantograph with respect to different values of d_S and K_S' are calculated and shown in Fig. 3 and Fig. 4. Figure 3 shows that both the mean contact force and standard deviation converge to standard values at d_S = 19 m, and they quickly increase with increasing and decreasing d_S. Figure 4 shows that both the mean contact force and standard deviation of the contact force decrease with

increasing K_S' and converge to the standard value when K_S' is greater than 7×10^5 N/m, which means that K_S' should be no less than 7×10^5 N/m to maintain the accuracy of the present model. Note that the original length of the stitch wire is 18 m in the EN50318-2018 standard, which means that the d_S should be slightly longer than the original stitch wire to ensure the accuracy of the present model. In addition, unlike the original MSM-based simple catenary model, the parameters of the stitch wire model in the present stitched catenary model further influence the calculation accuracy, which means that the stitch wire influences the dynamic responses of the whole catenary, and the stitch wire should be carefully modeled with proper parameters.

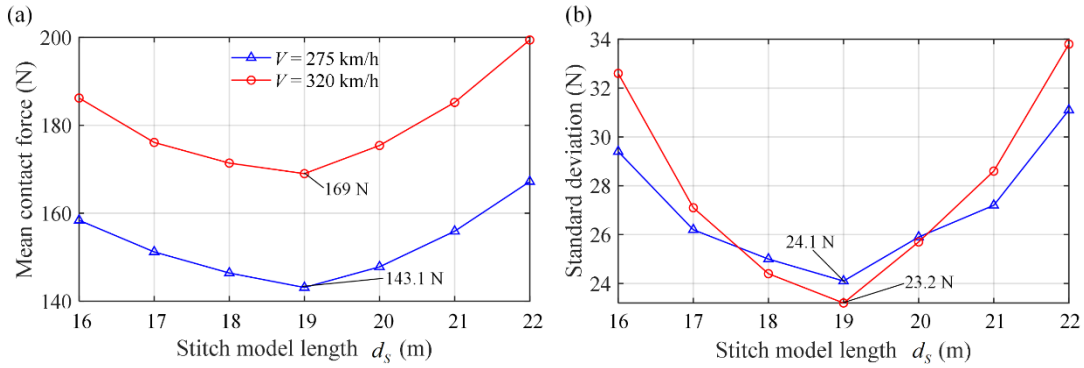

Fig. 3 Mean contact force and standard deviation of the contact force in the leading pantograph with respect to different d_S: (a) mean contact force and (b) standard deviation.

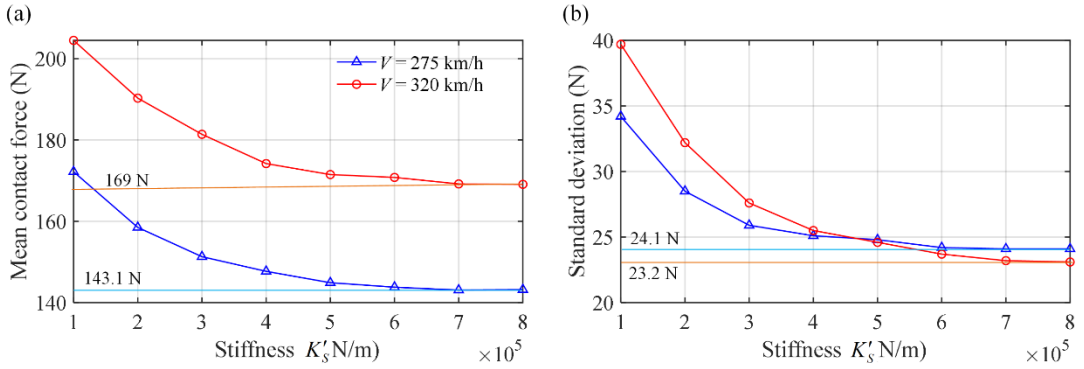

Fig. 4 Mean contact force and standard deviation of the contact force in the leading pantograph with respect to different K_S' values: (a) mean contact force and (b) standard deviation.

4 Conclusions and Contributions

In this study, an MSM-based pantograph–stitched catenary interaction model is developed to accurately and efficiently investigate the dynamic characteristics of pantograph–stitched catenary interactions. In the present model, a new stitched wire

model is developed, where the stitch wire and catenary suspension are simplified into a part of the messenger wire supported by a couple of spring-damper elements. The distance of these two spring-damper elements and the stiffness and damping of each spring-damping element are chosen to ensure that the stiffness of the stitch wire model is equal to the original stiffness. Then, the stitched catenary system with a simplified stitch wire model is modeled by MSM. The present model is validated with the EN 50318 standard, and the influence of different key parameters in the stitch wire model on the calculation accuracy is investigated.

Based on the obtained calculation results, the proposed MSM-based pantograph–stitched catenary interaction model can accurately investigate the dynamic behavior of pantograph–stitched catenary interactions. In the stitch wire model, the distance between every two spring-damping elements d_S and spring-damping element stiffness K_S' can strongly influence the calculation accuracy, which should be decided by pre-analysis method in different cases.

Acknowledgements

The authors would like to thank the support from the National Natural Science Foundation of China (grant number 12302048).

References

[1] A. Facchinetti, S. Bruni, “Hardware-in-the-loop hybrid simulation of pantograph-catenary interaction”, J Sound Vib, 331, 2783–2797, 2012.

[2] G. Bucca, A. Collina, “A procedure for the wear prediction of collector strip and contact wire in pantograph-catenary system”, Wear, 266, 46–59, 2009

[3] H. Yang, B. Hu, Y. Liu, X. Cui, G. Jiang, “Influence of reciprocating distance on the delamination wear of the carbon strip in pantograph–catenary system at high sliding-speed with strong electrical current”, Eng Fail Anal 104, 887–897, 2019.

[4] T. Ding, G.X. Chen, J. Bu, W.H. Zhang, “Effect of temperature and arc discharge on friction and wear behaviours of carbon strip/copper contact wire in pantograph-catenary systems”, Wear, 271, 1629–1636, 2011.

[5] H.J. Yang, G.X. Chen, G.Q. Gao, G.N. Wu, W.H. Zhang, “Experimental research on the friction and wear properties of a contact strip of a pantograph-catenary system at the sliding speed of 350km/h with electric current”, Wear 332–333, 949–955, 2015.

[6] T.J. Park, C.S. Han, J.H. Jang, “Dynamic sensitivity analysis for the pantograph of a high-speed rail vehicle”, J Sound Vib 266, 235–260, 2003.

[7] T.X. Wu, M.J. Brennan, “Basic analytical study of pantograph-catenary system dynamics”, Vehicle System Dynamics 30, 443–456, 1998.

[8] G. Poetsch, J. Evans, R. Meisinger, W. Kortüm, W. Baldauf, A. Veitl, J. Wallaschek, “Pantograph/catenary dynamics and control”, Vehicle System Dynamics 28, 159–195, 1997.

[9] M. Arnold, B. Simeon, “Pantograph and catenary dynamics: A benchmark problem and its numerical solution”, 2000.
[10] Y. Song, M. Zhang, O. Øiseth, A. Rønnquist, “Wind deflection analysis of railway catenary under crosswind based on nonlinear finite element model and wind tunnel test”, Mech Mach Theory, 168, 2022.
[11] J.P. Massat, C. Laurent, J.P. Bianchi, E. Balmès, “Pantograph catenary dynamic optimisation based on advanced multibody and finite element co-simulation tools”, Vehicle System Dynamics, 338–354, 2014.
[12] M. Tur, E. García, L. Baeza, F.J. Fuenmayor, “A 3D absolute nodal coordinate finite element model to compute the initial configuration of a railway catenary”, Eng Struct 71, 234–243, 2014.
[13] A. Facchinetti, S. Bruni, “Hardware-in-the-loop hybrid simulation of pantographcatenary interaction”, J Sound Vib 331, 2783–2797, 2012.
[14] A. Rønnquist, P. Nåvik, “Dynamic assessment of existing soft catenary systems using modal analysis to explore higher train velocities: A case study of a Norwegian contact line system”, Vehicle System Dynamics 53, 756–774, 2015.
[15] A. Facchinetti, L. Gasparetto, S. Bruni, “Real-time catenary models for the hardware-in-The-loop simulation of the pantograph-catenary interaction”, Vehicle System Dynamics 51, 499–516, 2013.
[16] Y. Yao, D. Zou, N. Zhou, G. Mei, J. Wang, W. Zhang, “A study on the mechanism of vehicle body vibration affecting the dynamic interaction in the pantograph–catenary system”, Vehicle System Dynamics 59, 1335–1354, 2021.
[17] Y. Xu, Z.D. Liu, S. Stichel, W.D. Zhu, J.L. Lei, Y. Yao, “A comparative study on the influence of typical track failures on high-speed pantograph-catenary interaction dynamics”, Vehicle System Dynamics, 2024.
[18] Z. Liu, P.A. Jönsson, S. Stichel, A. Rønnquist, “Implications of the operation of multiple pantographs on the soft catenary systems in Sweden”, Proc Inst Mech Eng F J Rail Rapid Transit 230, 971–983, 2016.